JOURNAL OF Applied Polymer SCIENCE

Enhancement of Weld Line Mechanical Strength Using a Novel Ejector-Pins Compression System

Shih-Chih Nian,[1] Ming-Shyan Huang[2]

[1]Department of Power Mechanical Engineering, National Taitung Junior College, 889 Jhengci N. Road, Taitung City 95045, Taiwan, Republic of China

[2]Department of Mechanical and Automation Engineering, National Kaohsiung First University of Science and Technology, 2 Jhuoyue Road, Nanzih, Kaohsiung City 81164, Taiwan, Republic of China

Correspondence to: S.-C. Nian (E-mail: lawrence@ntc.edu.tw)

ABSTRACT: This study proposes a novel ejector-pins compression system (EPCS) to improve the mechanical strength of weld lines that are formed in the injection molding process. Weld lines are significant defects that affect injection molding quality, causing the poor appearance and low mechanical strength of injection-molded parts. In this experiment, several ejector pins are placed intentionally near the weld lines appearing, and are initially sunken beneath the cavity surface to form a reflow trap such that some of the molten plastics are allowed to flow into it during the filling process. These molten plastics are then compressed by the arisen ejector pins. Accordingly, the compressed molten plastics reflow through the weld lines, disordering the molecular orientation. Experimental verification revealed that the use of an EPCS can efficiently eliminate the orientation of the molecules parallel to the weld line. The specimens' impact strength of using EPCS can increase to between one and two times than that of conventionally injection-molded. Therefore, this simple and novel method is feasible for greatly improving the mechanical strength of weld lines. © 2012 Wiley Periodicals, Inc. J. Appl. Polym. Sci. 000: 000–000, 2012

KEYWORDS: injection molding; weld line; ejector-pins compression system; molecular orientation

Received 7 May 2012; accepted 13 June 2012; published online
DOI: 10.1002/app.38207

INTRODUCTION

Injection molding is a process with low cost and high efficiency. It is therefore the most used manufacturing process in mass production. In the injection molding process, weld lines commonly appear and their formation is difficult to prevent. They are formed wherever two or more melt fronts meet in the filling stage when cavities have shut-off areas or injection-molding is performed using multi-gates. Weld lines are often visible on an injection-molded part and reduce their mechanical strength, because fountain flow produces parallel molecular orientations across weld lines and thereby cause weak intermolecular entangling forces.[1] Early studies on weld lines, Kim and Sun[2] established a theoretical model that offered comprehensive physical insight into bonding at the weld lines. The model was based on the self-diffusion of molecular chains across the polymer–polymer interface and the frozen-in orientation that remains parallel to the interface. It successfully predicted the strength of weld lines under given processing conditions and particular part geometry.

Weld lines are non-negligible defects that affect the quality of injection molding since they reduce the mechanical strength of injection-molded parts. The formation of weld lines is difficult to avoid completely, especially when cavities have shut-off areas or molding is carried out using multi-gates, but it can be minimized by controlling the part geometry, the locations of the gates, and the injection molding parameters.[3] Zhai and Au[4] presented a method for optimally locating weld lines by adjusting the locations of gates in a multi-gated injection molding system. Chen et al.[5] utilized fuzzy theory to control the location of weld lines by adjusting the location of gates and the thickness of parts. Wu et al.[6] proposed a distributed multi-population genetic algorithm that was combined with an optimization algorithm to be run in MoldFlow, a commercial simulation software package, to minimize the effects of weld lines. Xie et al.[7] used an overflow trap in the cavity and used a visualization system to examine the effect of the cavity geometry on weld lines. Their experimental results indicated that the overflow trap can change the location of weld lines and move these defects into an unimportant area. Chen et al.[8] developed a gas-driven sequential valve gate system for molding parts with thin walls. The system supported the rapid control of the sequence in which the gates are used to allow the melt to fill the cavity. The system

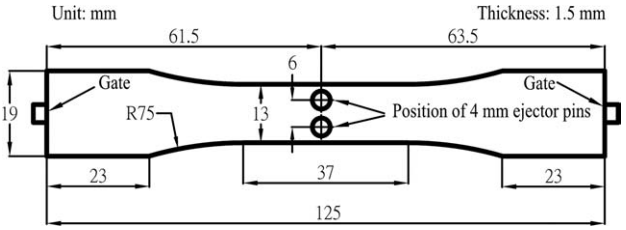

Figure 1. Geometry of tested specimens.

supported the molding of parts using multi-gates without the formation of weld lines, producing parts with superior cosmetic quality and better tensile strength.

Researchers have addressed the effect on weld lines of various process parameters, including melt temperature, mold temperature, injection speed, packing pressure, and gate location.[9–13] Moreover, design of experiment methods and finite element analysis have been adopted to optimize these process parameters to generate strong weld lines within injection-molded parts. For instance, Ozcelik[14] utilized the Taguchi L_9 orthogonal array to optimize the mechanical properties that are determined by weld lines on polypropylene (PP) specimens. He found that injection pressure and melt pressure are the most important process parameters in determining tensile strength and impact strength. Some researchers have employed dynamic mold surface temperature control systems[15,16] and cavity surface coating methods[17,18] to increase the temperature at which melt fronts merge, improving mechanical properties.

Even though the literatures on reducing or eliminating the effects of weld lines are extensive, no method based on disarranging the molecular orientation in weld lines to increase the strength of weld lines has been developed. This research proposes a novel and simple method, called the ejector-pins compression system (EPCS), to improve the mechanical strength of weld lines that are formed in the injection molding process. A dog bone-shaped cavity is formed using two gates and several motion ejector pins near the weld lines. The ejector pins are designed to sink beneath the surface of the cavity to enable it to store the reflow melt during mold filling. After the cavity is filled, the sunken ejector pins are lifted to compress the stored molten plastics reflow and then the parallel molecular orientation of the weld lines is disarranged. Three mechanical strength tests are performed to test tensile strength, flexural strength, and impact strength. The strength of weld lines produced using an EPCS is compared with that of those produced by conventional injection molding.

EXPERIMENTAL SETUP

Geometry and Material Properties of Specimen

In this investigation, a dog-bone shaped specimen referring to the test specimens of ASTM D638 standard was designed for the tests of mechanical strength. The specimen is 1.5 mm thick and 125 mm long. Figure 1 presents the detailed dimensions of the specimen that is used in the experiment.

To confirm the feasibility of the proposed method in improving the mechanical strength of weld lines, three polymers are used. They are (1) polystyrene (PS), which is hard and brittle and is made by Kaofulex Chemical (Specification: 525 N, Taiwan), (2) PP, which is flexible property and is made by Formosa Plastics (Specification: Yungsox 3204, Taiwan), and (3) acrylonitrile butadiene styrene (ABS), which has a high impact resistance, and is made by Chiemi (Specification: PA756, Taiwan).

Simulation and Tools

In this investigation, several sunken ejector pins near weld lines compress the molten plastics reflow after the cavity has been filled. When determining the diameters and positions of ejector pins of EPCS, several criteria have to be satisfied. (1) Control the location of weld lines at the edge of ejector pins to increase the effect of reflow-melt through the weld line interface. The design can also produce better air vents and less air trap. (2) The EPCS should provide enough pressure gradients to drive the compressed melt reflow through the weld line interface when the ejector pines were pushed forward. (3) The volume of compression melt determined by the ejector pines diameter and sunken depth should be suitable. It should be noted that little volume of compression melt would decrease the effect of EPCS and an excess of compression melt would produce over-packing injection molded parts and thus causes additional residual stress. In this study, the effects of ejector pins varying the diameters, locations, and sunken depths on the shape and location of weld lines are simulated using the commercial software Moldex3D R9.1. The forthcoming experiments were conducted on an all-electric injection molding machine (HE-50, Fu Chun Shin, Taiwan) with a clamping force of 50 tons, whose specifications are listed in Table I.

Mold Design and Process Parameter Settings

In this experiment, two edge gates, one at each end of the specimen, were designed to cause the melt fronts to collide and form weld lines. Near the weld lines, two motion ejector pins were sunken to store and compress the reflow melt. The diameters, sunken depth, and positions of the ejector pins were determined from the CAE simulation. In this investigation, ejector pins with a diameter of 4 mm and a sunken distance of 1 mm were used in the compression process. Figure 1 displays the positions of the pins.

Three types of specimen were formed using different molding processes and compared. They were: (1) free of weld lines, formed by single-gate cavity and conventional injection molding, ("no weld line"); (2) with weld lines, formed by two gates cavity and conventional injection molding, ("IM"); (3) with weld lines,

Table I. Specifications of FCS HE-50 Injection Molding Machine

Main items	Unit	Value
Screw diameter	mm	22
Maximal injection pressure	kgf/cm^2	2224
Theoretical shot volume	cm^3	42
Maximal shot weight (PS)	gram	38
Maximal injection speed	mm/s	300
Maximal injection stroke	mm	110
Clamping force	Tonf	50

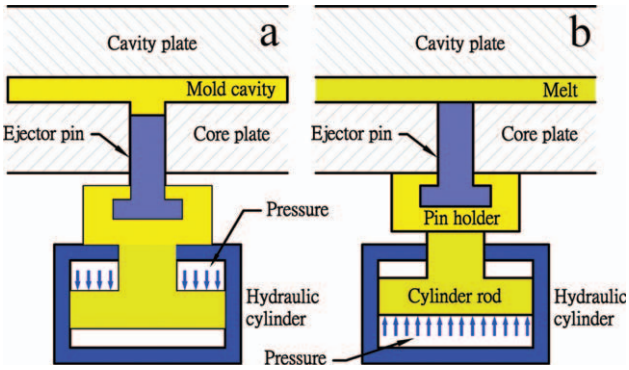

Figure 2. IM-EPCS: (a) ejector pins are drawn back and (b) ejector pins are pushed to compress resins. [Color figure can be viewed in the online issue, which is available at wileyonlinelibrary.com.]

formed by two gates cavity and EPCS-aided injection molding, ("IM-EPCS"). Figure 2 schematically depicts injection molding using an EPCS. The ejector pins were sunken beneath the cavity surface to form a reflow trap area by a hydraulic cylinder before the melt was injected [Figure 2(a)]. After the cavity was filled, the hydraulic cylinder pushed the ejector pins to compress the stored melt plastics, causing it to reflow into the cavity [Figure 2(b)]. The reflowed melt destroyed the molecular orientation along the weld lines, improving their mechanical strength.

The EPCS-aided injection molding process is composed of eight stages: (1) drawing back of ejector pins, (2) closing of mold, (3) filling of cavity, (4) low-pressure packing, (5) pushing of ejector pins to compress the stored melt reflow, (6) high-pressure packing, (7) cooling, and (8) opening of mold and ejecting of parts.

In this investigation, three materials—PS, PP, and ABS—were used to examine the effects of an EPCS on the strengths of weld lines. Table II presents their injection molding parameters.

Mechanical Strength Tests

The standard tests of the mechanical strength of a plastic specimen determine their tensile properties, flexural properties, and impact resistance. In this investigation, all three tests were used to examine the effects of introducing an EPCS into injection

Table II. Set Process Parameters for Injection Molding Using PS, PP, and ABS Resins

Process parameter settings	Materials		
	PS	PP	ABS
Melt temperature (°C)	210	230	230
Mold temperature (°C)	40	40	40
Injection speed (mm/s)	40	40	50
Two-staged packing setting			
Packing pressure stage 1/Stage 2 (kgf/cm^2)	255/408	255/408	255/408
Packing time stage 1/Stage 2 (s)	1/5	1/7	1/6
Cooling time (s)	40	40	40

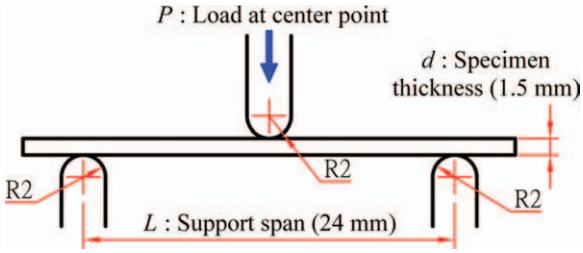

Figure 3. Dimensions of fixture in flexural test. [Color figure can be viewed in the online issue, which is available at wileyonlinelibrary.com.]

molding. The experimental setup and procedures referred to the standard test for the tensile properties of plastics (ASTM D638), the standard test for the flexural properties of unreinforced and reinforced plastics and electrical insulating materials (ASTM D790), and the standard test for determining the Izod pendulum impact resistance of plastics (ASTM D256).

In the experimental test, a commercial tensile testing machine (HT-2102AP, Huang-Ta, Taiwan) was adopted to obtain the tensile stress-strain diagram. Flexural and Izod impact tests were carried out using flexural and Izod impact testing machines that were made in the laboratory. The impact energy was measured by using an Izod impact test. The curves of flexural stress, σ_f, versus flexural strain, ε_f, were obtained by performing the flexural test. Figure 3 presents the dimensions of the fixture that was used in the flexural test. Equations (1) and (2) define σ_f and ε_f, respectively.

$$\sigma_f = \frac{3PL}{2bd^2} \tag{1}$$

$$\varepsilon_f = \frac{6Dd}{L^2} \tag{2}$$

where P denotes the load, L is the distance between supports, b is the width of the tested beam, d is the thickness of the specimen, and D is the maximal deflection of the beam.

RESULTS AND DISCUSSION

Analysis of CAE Simulation

Initially, various arrangements of ejector pins versus the formed weld lines were simulated. These simulations were conducted to determine the ideal diameters and positions of ejector pins for

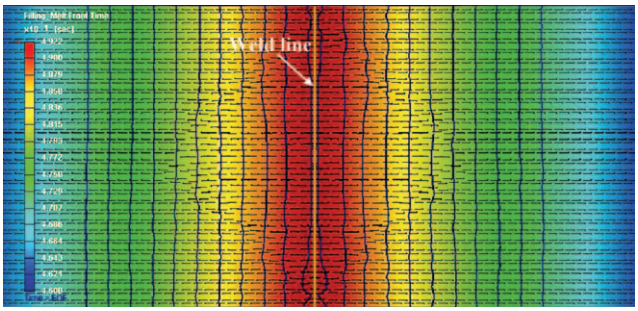

Figure 4. Linear weld line formed in conventional injection molding process. [Color figure can be viewed in the online issue, which is available at wileyonlinelibrary.com.]

Applied Polymer SCIENCE

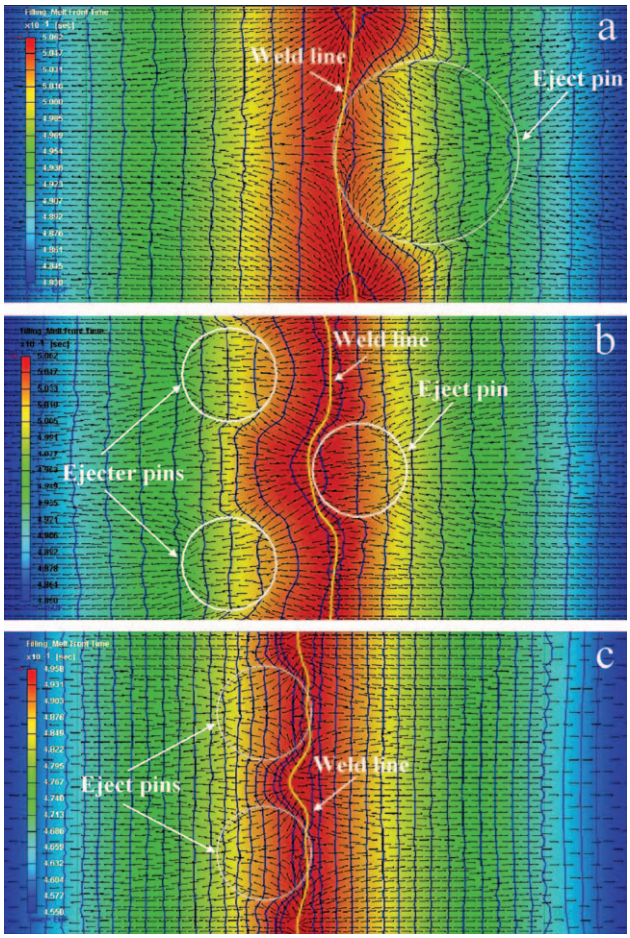

Figure 5. Various curved weld lines formed in injection molding process with EPCS: (a) one large ejector pin, (b, c) two ejector pins, and (d) three ejector pins. [Color figure can be viewed in the online issue, which is available at wileyonlinelibrary.com.]

use in the subsequent experiment. Figure 4 presents the melt flow behaviors in a conventional injection molding process, especially at the moment of formation of weld lines, when the melt fronts directly collide with each other, forming straight weld lines. The directly colliding weld lines have smallest melt front contact angles and therefore lower merge strength.[1,12]

Figure 5 displays the results of the simulated melt front time, weld line, and velocity vector for three mold designs with sunken ejector pins, with the sunken depth set to 1 mm. A thicker cavity generated with the sunken ejector pins reduces flow resistance of the melt and led to the ahead of melt front. The ahead melt front was helped to prevent it from directly colliding with other melt fronts, increasing its contact angle. A larger contact angle promotes the merging of the melt front, yielding a stronger weld line.[1,12] The contact angle is also examined by simulating the velocity vector. Curved weld lines help to reduce the effects of stress concentration during flexure and impact tests. Also, arranging the ejector pins near the weld line makes the air vents more effective in the filling stage.

Figure 5(a) shows the simulated weld line of using one large-diameter ejector pin to perform the EPCS process. The large ejector pin could store major reflow melt and provide larger pressure gradient to drive more melt to reflow through the weld line interface. However, this large ejector pin might generate too much compression and then result in over-packing. Figure 5(b) shows the simulation results of ejector pins located at the both sides of weld lines. Figure 6 shows the birefringence patterns of PS specimens proceeded with the IM-EPCS processes. Figure 6 depicts that the design was poor since the pressure at the both sides of weld lines increase immediately as the ejector pines pushing forward. The pressure gradients thus would drive the compression melt flowing to the gate direction which is in the lower pressure region, such that the reflow melt would not across the weld line. In contrast, Figure 5(c) shows better

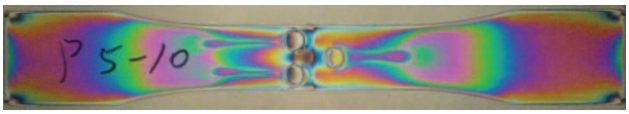

Figure 6. Birefringence of specimens with three ejector pins made of PS resins. [Color figure can be viewed in the online issue, which is available at wileyonlinelibrary.com.]

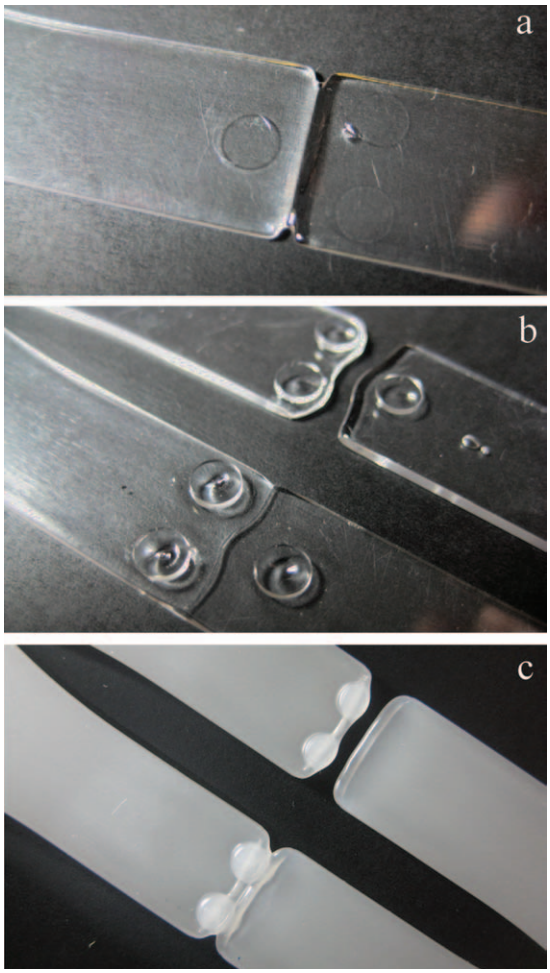

Figure 7. Various curved weld lines formed in injection molding process with EPCS: (a) without sunken ejector pin, (b) with three sunken ejector pins, and (c) with two sunken ejector pins. [Color figure can be viewed in the online issue, which is available at wileyonlinelibrary.com.]

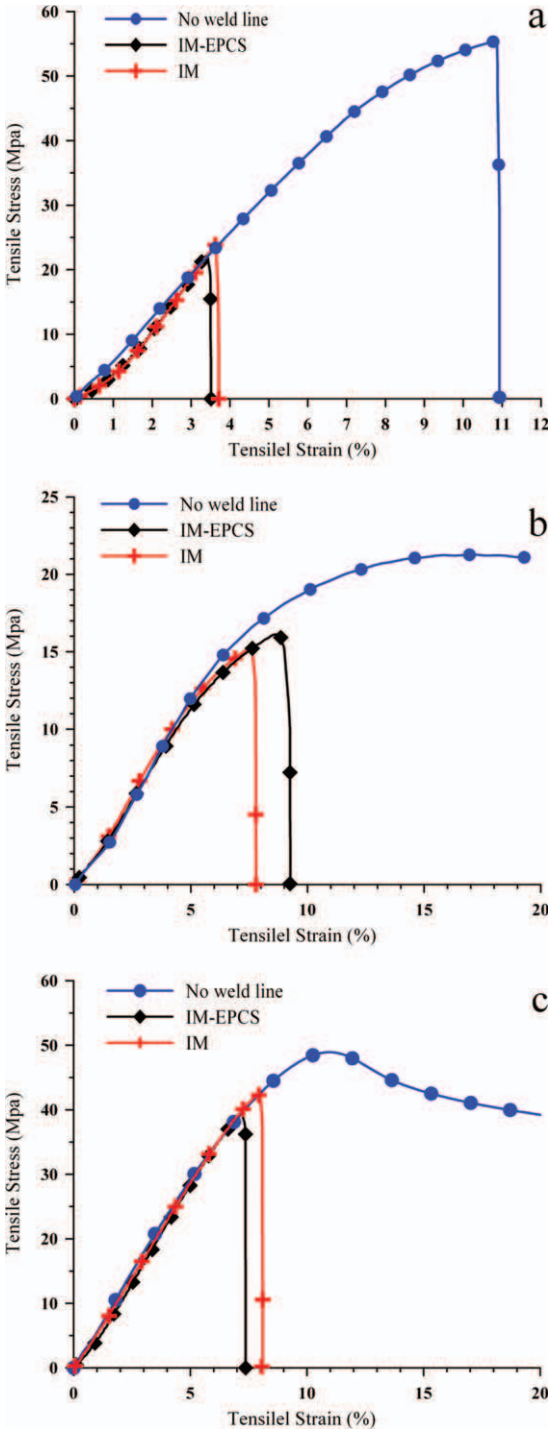

Figure 8. Tensile stress versus tensile strain for various plastic materials: (a) PS resins, (b) PP resins, and (c) ABS resins. [Color figure can be viewed in the online issue, which is available at wileyonlinelibrary.com.]

performance of EPCS and the design is adopted in the subsequent experiment. Figure 7(a) shows the short-shoot specimen formed by the conventional injection molding process, in which the melt fronts come into contact and merge as a straight line. Figure 7(b, c) presents the short-shoot specimens with three and two sunken ejector pins, respectively. The curved melt fronts that are formed by the sunken ejector pins clearly meet to form a curved shape weld line.

Tensile Strength of Weld Lines

Tensile tests were conducted on specimens formed using different molding processes. Figure 8(a–c) plots tensile stress versus tensile strain for the PS, PP, and ABS materials, respectively. The test results showed that the existence of weld lines significantly reduced the tensile strength of specimens—especially those made of the PS material. The use of an EPCS in injection molding had only a limited effect on the maximal tensile stress and tensile strain. The EPCS was observed slightly to increase the tensile strength of specimens that were made of PP, which is a flexible material, but it reduced that of the specimens that were made of ABS and PS. The drop in tensile strength was thought to have been caused by an increase in residual stress, which was itself generated by the compression using the EPCS. Figure 9 presents the birefringence of PS specimens made by the IM and IM-EPCS processes. The birefringence patterns demonstrate that the EPCS increased the residual stress around the weld lines and reduced the tensile strength.

Flexural Strength of Weld Lines

Figure 10(a–c) plots the flexural stress versus flexural strain for specimens that were made of PS, PP, and ABS, respectively. Table III summarizes the maximal flexural stress and the corresponding flexural strain of the test results. The results showed that the weld lines substantially affected the flexural strength—especially of the hard and brittle material PS. The EPCS improved the maximum flexural stress and flexural strain of the weld lines in all of the experimental materials. To elucidate the effects of the EPCS on flexural destruction, the cross-sections of the destroyed specimens were observed and discussed.

Figure 11 displays the cross-sections of destroyed IM and IM-EPCS specimens of PS. The IM specimen had a uniform destructive section along the weld lines. However, the destroyed IM-EPCS specimen exhibited an irregular cross-section. These results imply that the EPCS successfully compressed the melt reflow, eliminating the parallel arrangement of the molecules along the interface of weld lines, forming an irregular destructive section. The EPCS efficiently increased the maximum flexural stress of the PS specimens by 46% (from 36.3 to 53.1 MPa) and the corresponding flexural strain by 52% (from 2.3 to 3.5%).

Figure 12(a, b) presents the top-view and back-view of the bent PP specimens, respectively. They indicate that the specimen without weld lines had the largest bending deformation region

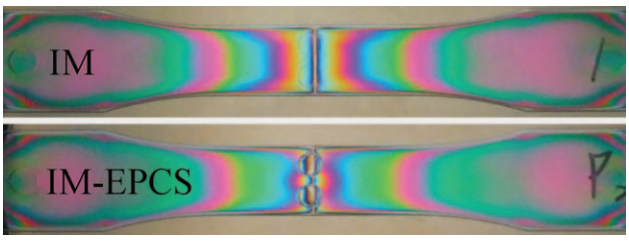

Figure 9. Birefringence of specimens made of PS resins. [Color figure can be viewed in the online issue, which is available at wileyonlinelibrary.com.]

Applied Polymer SCIENCE

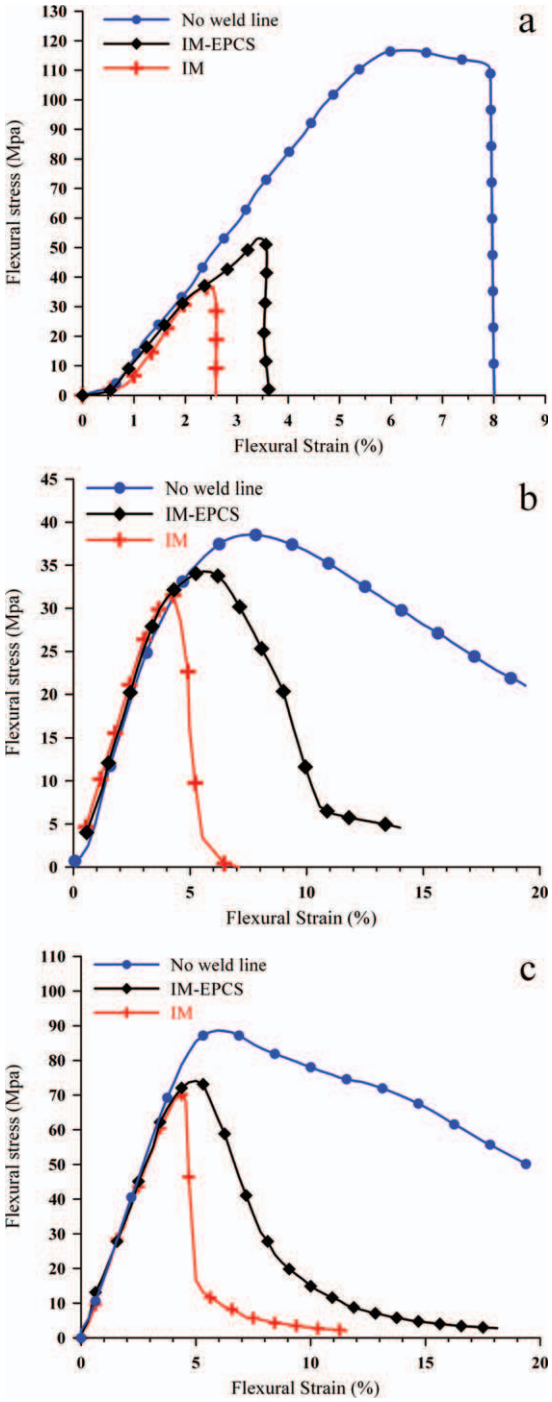

Figure 10. Flexural stress versus flexural strain for various plastic materials: (a) PS resins, (b) PP resins, and (c) ABS resins. [Color figure can be viewed in the online issue, which is available at wileyonlinelibrary.com.]

and had no cracking on its surface. In contrast, the IM specimen exhibited a straight flat surface of cracks on the weld lines [Figure 12(a)]. An obvious concentration of stress is evident around the crack in the flexural test, resulting in a narrow and straight band of deformation [Figure 12(b)]. The crack in the specimen that exhibited weld lines that was formed by the EPCS was curved and irregular [Figure 12(a)], and the deformation band was curved and larger [Figure 12(b)] than that of the

Table III. Results of Flexural Tests

	Max. flexural stress (MPa)			Flexural strain (%)		
Materials	No. weld line	IM	EPCS	No. weld line	IM	EPCS
PS	116.7	36.3	53.1	6.2	2.3	3.5
PP	38.6	32.1	34.7	7.5	4.6	5.9
ABS	88.7	70	74	5.9	4.4	5.3

IM specimen. A more curved and larger deformation band was associated with a higher maximal flexural stress and strain. The deformation band was larger because of the curved weld line and the reflowed melt, which were generated by the sunken ejector pins and the pushed ejector pins, respectively. A curved weld line dispersed the bending force, reducing the stress concentration. The reflowed melt eliminated the arrangement of parallel molecules along the interface of weld lines, preventing them from being torn apart directly on the interface between merged melt fronts. Figure 12(c, d) presents the cross-sections of destroyed IM and IM-EPCS specimens of PP, respectively. The destroyed IM specimen also yielded a uniform section along the weld lines. The cross-sections of the destroyed IM-EPCS specimens were of three types. (1) The first type exhibited a uniform broken area near the top and side surfaces of the specimen (see marked area), in the frozen layer (in contact with the wall of the mold), through which the reflow melt does not flow and in which the parallel molecular orientation is not

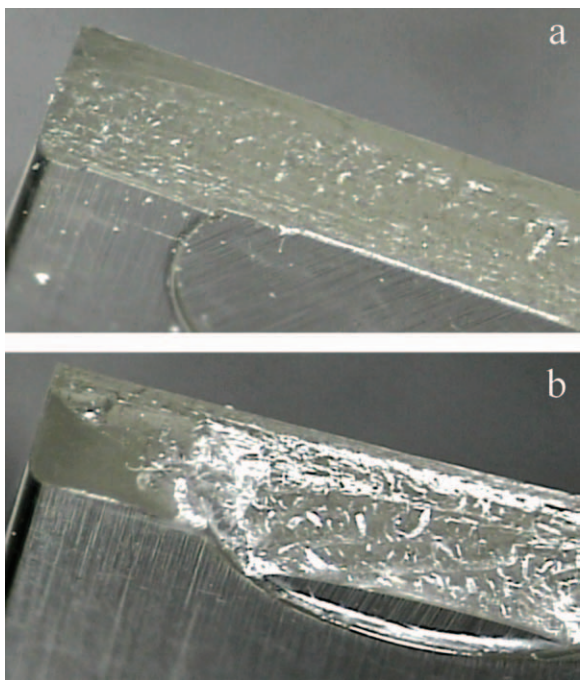

Figure 11. Cross-sections of PS specimens along weld lines: (a) IM and (b) IM-EPCS. [Color figure can be viewed in the online issue, which is available at wileyonlinelibrary.com.]

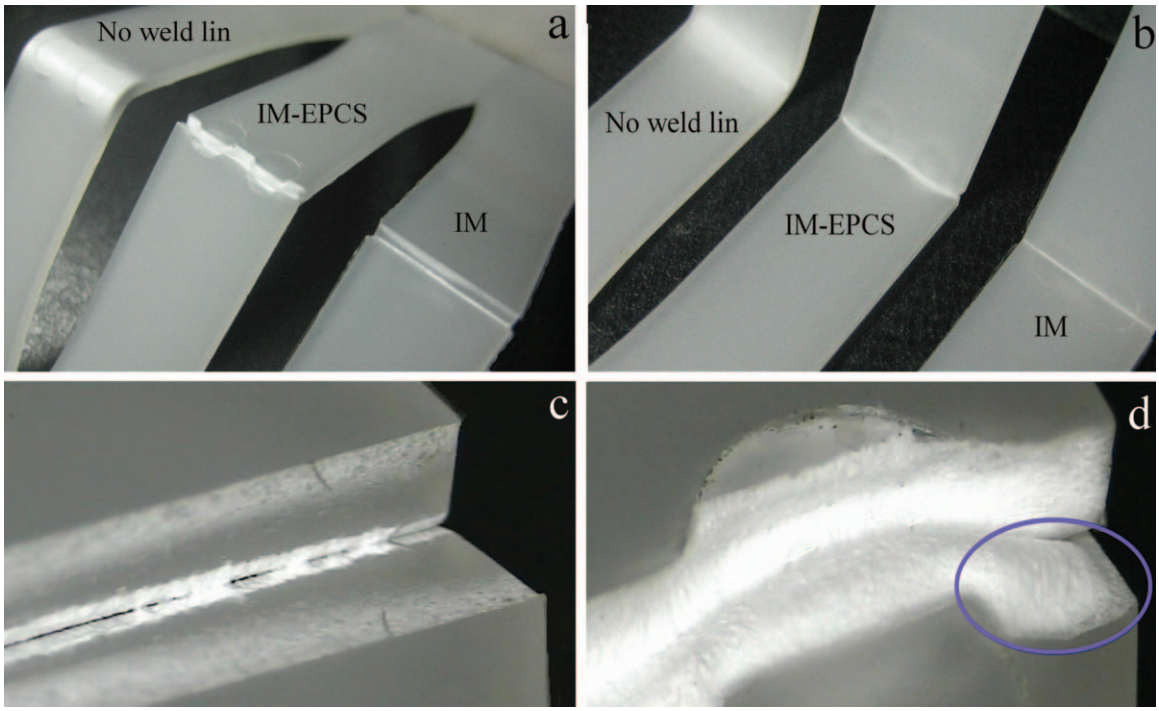

Figure 12. Weld lines of PP specimens: (a) top view, (b) back view, (c) IM, and (d) IM-EPCS. [Color figure can be viewed in the online issue, which is available at wileyonlinelibrary.com.]

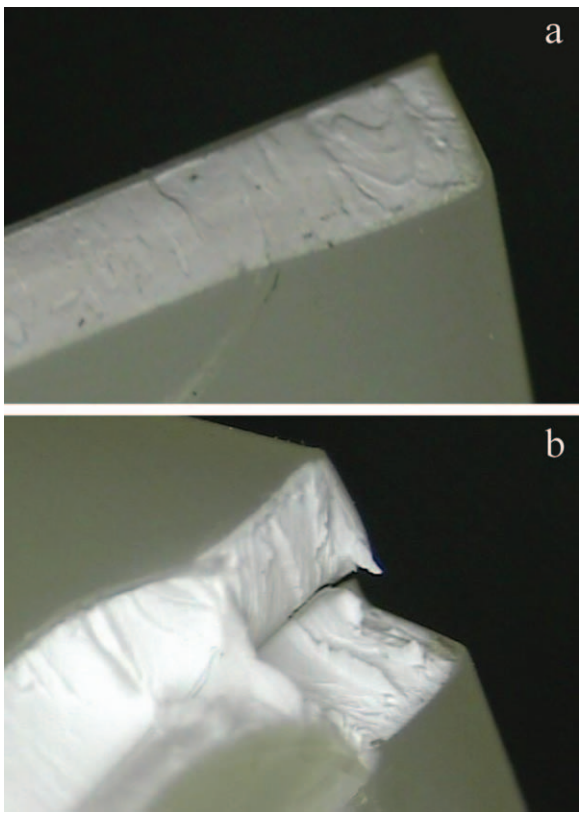

Figure 13. Weld lines of ABS specimens: (a) IM and (b) IM-EPCS. [Color figure can be viewed in the online issue, which is available at wileyonlinelibrary.com.]

eliminated. (2) The second type exhibited an elongated area of deformation on the bottom surface of specimen, connecting both sides of the destroyed specimen and preventing it from being completely broken (3) The third type exhibited a tensional fracture area between the broken area and the elongated deformation area in which the cross-section of reflow melt pass through and the resin was fractured by the tensile stress of bending. The proposed EPCS increased the maximal flexural stress in the PP specimen by 8.1% (from 32.1 to 34.7 MPa) and the flexural strain by 28% (from 4.6 to 5.9%) [Table III and Figure 10(b)].

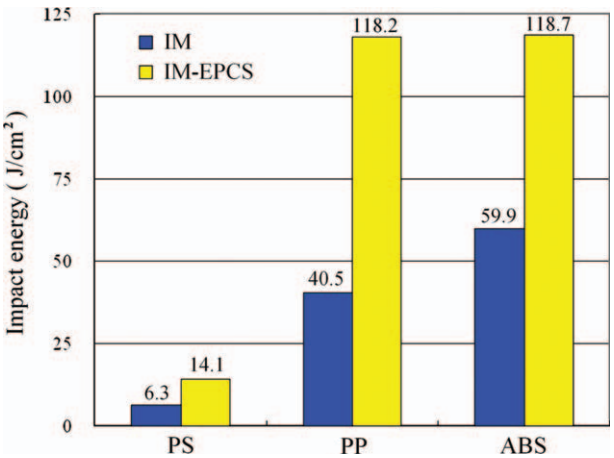

Figure 14. Impact energies of IM and IM-EPCS specimens. [Color figure can be viewed in the online issue, which is available at wileyonlinelibrary.com.]

Figure 13(a, b) displays the cross-section of the destroyed IM and IM-EPCS specimens of ABS, respectively. The IM specimens of ABS, like the PP specimens, exhibited a straight and flat crack along the weld lines. However, the ABS specimens with the EPCS exhibited different destructive phenomena. The broken cross-section of the IM-EPCS specimen also included a uniform broken area near the top and side surfaces of the specimen, but without the elongated deformation area. In other areas, the resin was irregularly torn at breakage. The proposed EPCS increased the maximal flexural stress of the ABS specimens by 5.7% (from 70 to 74 MPa) and their flexural strain by 20% (from 4.4 to 5.3%) [Figure 10(c) and Table III].

Impact Strength of Weld Lines

The impact strength test reveals the ability of a specimen to endure a sudden impact, which is an important property of injection-molded parts that are used in structures. Figure 14 presents the impact energy of PS, PP, and ABS specimens along weld lines with IM and IM-EPCS. Specimens that were molded with the EPCS exhibited significantly improved impact strength over that of those molded without an EPCS. The variation in impact energy variations was consistent with the measured area under the stress–strain curves (Figure 10). The area under the flexural stress–strain curve was a measure of a specimen's ability to absorb energy in the bending process. The area variation among the flexural stress–strain diagrams (Figure 10) demonstrates that the increases in both the maximal flexural stress and the flexural strain increased the area, and using the EPCS in the IM process greatly increased. The proposed EPCS increased impact strengths of the PS, PP, and ABS specimens by 124% (from 6.3 to 14.1 J/cm^2), 192% (from 40.5 to 118.2 J/cm^2), and 98% (from 59.9 to 118.7 J/cm^2), respectively. These results confirm that the proposed EPCS feasibly and significantly reduced the loss of impact strength that was caused by weld lines.

CONCLUSION

This study successfully developed an EPCS to improve the mechanical strength of parts with weld lines in injection molding. All of the main tests of mechanical strength of a plastic specimen, which reveal tensile properties, flexural properties, and impact resistance, were performed to examine the effects of using an EPCS in injection molding. The effects of the EPCS on different types of polymer, such as the hard and brittle PS, the flexible PP, and the ABS with high impact resistance, were studied. The simulation and experimental results demonstrate that injection molding with EPCS can successfully curve the weld line, increasing contact angle of the melt front, and drive the melt reflow through the weld lines. The curving of the weld line reduces the effects of stress concentration; a larger contact angle corresponds to greater strength upon merging of the melt, and the reflow melt can efficiently solve the problem of molecular orientation at the weld line interface. The results of the mechanical strength tests reveal that the use of the EPCS significantly improves the flexural and impact strengths of weld lines, but has only a slight effect in tensile strength. The EPCS can slightly increase the tensile strength of PP specimens, but it slightly reduced those specimens of ABS and PS. In the flexural test, the proposed EPCS increased the maximal flexural stress of the PS, PP, and ABS specimens by 46, 8.1, and 5.7%, respectively, and the flexural strain by 28, 52, and 20%. In particular, the EPCS greatly increased the impact strength of the PS, PP, and ABS specimens by 124, 192, and 98%, respectively. All of the results of this investigation confirm that the EPCS is a feasible and efficient system for reducing the loss of mechanical strength that is caused by weld lines.

ACKNOWLEDGMENTS

The authors thank the Fu Chun Shin Machinery Manufacture and the Precision Mold and Die Research and Development Center for providing assistance with the experimental equipments and molding technology. Ted Knoy is appreciated for his editorial assistance.

REFERENCES

1. Kobayashi, Y.; Teramoto, G.; Kanai, T. *Polym. Eng. Sci.* **2011,** *51*, 526.
2. Kim, S. G.; Suh, N. P. *Polym. Eng. Sci.* **1986,** *26*, 1200.
3. Kovács, J. G.; Sikló, B. *Polym. Test.* **2010,** *29*, 910.
4. Zhai, M.; Lam, Y. C.; Au, C. K. *Eng. Comput.* **2006,** *21*, 218.
5. Chen, M. Y.; Tzeng, H. W.; Chen, Y. C.; Chen, S. C. *ISA Transaction.* **2008,** *47*, 119.
6. Wu, C. Y.; Ku, C. C.; Pai, H. Y. *Int. J. Adv. Manuf. Tech.* **2011,** *52*, 131.
7. Xie, P. C.; Du, B.; Yan, Z. Y.; Ding, Y. M.; Yang, W. M. *Adv. Matres.* **2010,** *87/88*, 31.
8. Chen, S. C.; Chien, R. D.; Tseng, H. H.; Huang, J. S. *J. Appl. Polym. Sci.* **2005,** *98*, 1969.
9. Chang, T. C.;Faison, E., III. *J. Inject. Mold. Technol.* **1999,** *3*, 61.
10. Liu, S. J.; Wu, J. Y.; Chang, J.-H.; Hung, S. W. *Polym. Eng. Sci.* **2000,** *40*, 1256.
11. Wu, C. H.; Liang, W. J. *Polym. Eng. Sci.* **2005,** *45*, 1021.
12. Ozcelik, B.; Kuram, E.; Topal, M. *Int. Commun. Heat Mass* **2012,** *39*, 275.
13. Chen, S. C.; Lid, H. M.; Hsue, P. M.; Penge, H. S. *Polym. Plast. Technol.* **2011,** *50*, 276.
14. B. Ozcelik, *Int. Commun. Heat Mass* **2011,** *38*, 1067.
15. Chen, S. C.; Jong, W. R.; Chang, J. A. *J. Appl. Polym. Sci.* **2006,** *101*, 1174.
16. Xie, L.; Ziegmann, G. *Microsyst. Technol.* **2007,** *14*, 809.
17. Xie, L.; Ziegmann, G.; Hlavac, M.; Wittmer, R. *Microsyst. Technol.* **2010,** *16*, 1009.
18. Chen S. C.; Chang, Y.; Chang, Y. P.; Chen, Y. C.; Tseng, C. Y. *Int. Commun. Heat Mass* **2009,** *36*, 1030.